Catalysis Letters, Vol. 114, Nos. 1–2, March 2007 (© 2007)
DOI: 10.1007/s10562-007-9046-4

Selective catalytic low pressure hydrogenation of acetophenone on $Pd/ZnO/ZnAl_2O_4$

Maurizio Lenarda,[a,]* Manuela Casagrande,[a] Elisa Moretti,[a] Loretta Storaro,[a] Romana Frattini,[b] and Stefano Polizzi[b]

[a]*INSTM UdR di Venezia, Dipartimento di Chimica, Università Ca' Foscari, di Venezia, Via Torino 155/B, Mestre, VE 30172, Italy*
[b]*INSTM UdR di Venezia, Dipartimento di Chimica-Fisica, Università di Venezia Ca' Foscari, Via Torino 155/B, Mestre, VE 30172, Italy*

Received 5 December 2006; accepted 4 January 2007

A PdZn alloy-based catalyst was prepared by impregnation with a Pd salt of the oxides obtained by the thermal decomposition of a Zn–Al hydrotalcite. Two samples were obtained by carrying out the reduction at 373 and 673 K, that were characterized by chemical analysis, powder XRD and TEM. The catalytic activity was tested in the low pressure hydrogenation of acetophenone. The results were compared with those obtained using a conventional palladium catalyst.

KEY WORDS: PdZn alloy; bimetallics; hydrogenation; acetophenone; hydrotalcite.

1. Introduction

Palladium based catalysts are largely used in the hydrogenation of organic substrates [1–4]. The properties of palladium based heterogeneous catalysts can be easily modified in order to increase selectivity by the presence of a second component and the alterations induced by alloying have been recently reviewed [2]. Various authors have observed that the catalytic behavior of Pd in a reductive atmosphere is significantly modified when ZnO is used as a support and the catalyst is pretreated at high temperature in hydrogen flow before use [5–10]. In fact, when a Pd/ZnO catalyst is reduced in hydrogen flow above 553 K a significant reduction of ZnO is observed, along with the formation of PdZn intermetallic alloys generated by the interaction of reduced Zn with metallic Pd [8–13]. The temperature of the reduction process influences the amount of metallic alloys [8–13] and consequently the Pd/PdZn ratio.

Layered hydrotalcite-like anionic clays (HTlc), of general molecular formula $M_x^{2+}M_y^{3+}(OH)_{2(x+y)}A_{y/n}^{-n}\cdot mH_2O$ where M^{2+} and M^{3+} are divalent and trivalent metal ions, respectively and A^{-n} is an intercalated anion, are widely used as catalysts or catalyst precursors [14–16]. In fact, thermal treatment of HT-like materials at high temperatures produces mixed oxides of well defined and reproducible stoichiometry [14, 15].

The thermal treatment of a $M^{2+}M^{3+}$ hydrotalcite above 1173 K is known to lead to the complete decomposition of the layered structure with formation of $M^{2+}O$ and a spinel-type phase ($M^{2+}M_2^{3+}O_4$) [14, 15].

In this study we describe the preparation of two Pd-based catalyst samples obtained by impregnation with a palladium salt the mixture of oxides generated by thermal decomposition above 1173 K of an Zn–Al HTlc. The impregnated samples were successively reduced with H_2 at two different temperatures. The catalytic behavior of the two samples was tested in the reduction of acetophenone with hydrogen in batch conditions. The reaction was selected not only because the catalytic reduction of aromatic ketones is important in the synthesis of fine chemicals, pharmaceuticals and cosmetics, but also because the complex pattern of this multistep reaction can be a useful tool, to test the activity and selectivity properties of a catalytic system. While various monometallic catalytic systems based on supported precious metals [17–29] have been successfully used in the hydrogenation of acetophenone, both in batch and in vapor flow reactors, bimetallic systems, [26–29], have shown superior stability and selectivity.

2. Experimental

2.1. Catalyst preparation

A Zn–Al hydrotalcite (HTZAas) sample was obtained by precipitation of the hydroxycarbonates from a solution containing the metal chlorides and urea following a procedure described by Costantino et al. [30]. Solid urea was added to a 0.5 M metal chloride solution, with a molar fraction Al/(Al + Zn) = 0.33, until a urea/metal chloride molar ratio value of 3.3 was

---

*To whom correspondence should be addressed.
E-mail: lenarda@unive.it

reached. The solution was heated, under vigorous stirring, at 263 K for 40 h. The white precipitate was recovered by filtration, washed with distilled water until complete the disappearance of chloride ions (silver nitrate test).

The resulting material was dried at 353 K and successively calcined at 1173 K for 12 h till the complete decomposition of the layered structure to a mixture of ZnO and of a spinel-type ($ZnAl_2O_4$) phase (HTZA).

HTZA was successively impregnated with an aqueous solution of $Pd(NO_3)_2 \cdot nH_2O$ to reach a palladium loading of 2%w/w. The resulting material was slit into two samples that were both calcined for 2 h at 623 K and then reduced in hydrogen flow (40 mL/min), one at 373 K and the other at 673 K, (heating rate of 5 K/min) for 2 h. The obtained catalysts were named HTZAPd373 and HTZAPd673, respectively.

For the sake of comparison a conventional Pd/C sample was prepared by impregnation with the nitrate salt and reduced in H_2 flow at 673 K for 2 h.

2.2. *Powder X-ray diffraction (XRD)*

The X-ray diffraction patterns were collected with a Bragg-Brentano powder diffractometer using the CuKλ radiation (λ = 1.5418 Å) and a graphite monochromator. Diffraction data were analyzed using the Rietveld method [31] and the MAUD codes [32]. This program, in a fully automated version, is particularly suited for a quantitative evaluation of the phases present in the X-ray diffraction patterns. Physical parameters such as average crystallite size are deduced from the full pattern analysis and not by comparative investigation of the peak broadening after the analysis of each peak [32].

2.3. *Transmission electron microscopy*

Transmission electron micrographs were taken on a JEOL-JEM 3010 microscope, equipped with lanthanum hexaboride (LaB_6) gun, using an accelerating voltage of 300 kV. The images were taken with a slow-scan CCD camera (Gatan, mod. 694).

2.4. *Catalytic hydrogenation of acetophenone*

The hydrogenation of acetophenone was carried out in a 200 mL stainless steel autoclave. The reactor was charged with 100 mg of catalyst, 10 mL of *n*-hexane and 0.5 mL of acetophenone. The vessel was purged with hydrogen three times, pressurized up to 9 bar and finally heated to the fixed temperature. The stirring was maintained at about 500 rpm.

After the required reaction time the reactor was cooled to room temperature and the reaction mixture filtered and analyzed by GC-MS and GC.

The analysis was carried out with a Hewlett Packard 6890 GC equipped with a FID detector and a HP-5 capillary column and by GC-MS with a Hewlett Packard G1800C apparatus.

3. Results and discussion

3.1. *Catalyst characterization*

3.1.1. *X-ray powder diffraction (XRD)*

XRD was used to follow the structural modifications of the catalyst samples during the preparation. The XRD profile of the starting layered double oxide is typical of a well crystallized hydrotalcite (HT) phase. On the other hand, the diffraction pattern of the material after thermal treatment at 1173 K (HTZA) is a combination of the typical reflections of crystalline ZnO and of a spinel-type ($ZnAl_2O_4$) phase.

Figure 1 shows the experimental XRD pattern of HTZAPd373 along with the fit obtained using the Rietveld method. A very broad and asymmetric peak centered at about $2\theta = 40.5°$ was detected in the XRD profile, in addition to the peaks of the $ZnAl_2O_4$ and ZnO phases. It was impossible to explain the asymmetry of the peak supposing only the presence of a nanocrystalline Pd phase and therefore it was necessary to also consider the existence of the tetragonal 1:1 PdZn alloy. In fact, the very broad peak could be only fitted if both phases were used.

It is very difficult to give a precise quantitative evaluation of the amount of PdZn alloy present because the particle dimensions are below the detectability limits and the secondary reflections of Pd and PdZn phases are hidden by those of the $ZnAl_2O_4$ and ZnO. Nevertheless we can suppose the presence of a substantial amount of

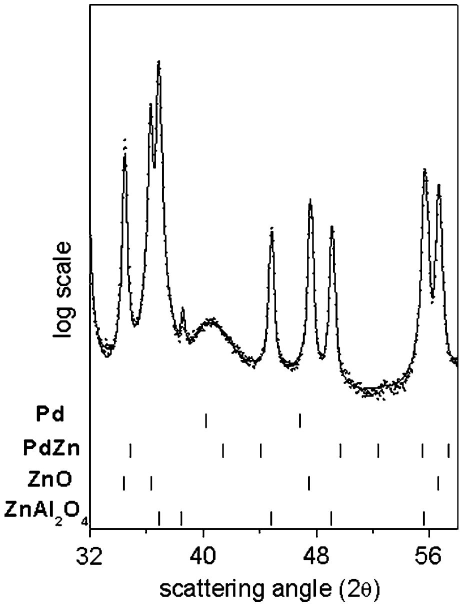

Figure 1. X-ray diffraction patterns (logarithmic scale) versus 2θ of HTZAPd373. Data points refer to experimental data and full lines to a curve fit according to the Rietveld methods.

tetragonal 1:1 PdZn alloy with particles smaller than 2 nm.

Palladium and zinc are known to be very miscible and can easily form an alloy when a mixture of the two metals is thermally treated in a reducing atmosphere [2] or if an intimate mixture of zinc oxide and palladium is reduced at high temperature in hydrogen flow. The tendency of the two metals to form an alloy increases with the increasing reduction temperature as reported by other authors [7–13].

Increasing the reduction temperature of the catalyst up to 673 K (sample HTZAPd673) the formation of the PdZn alloy is almost complete and alloy crystallites, of an average dimension of 9 nm, were formed.

The XRD pattern of this sample (figure 2) shows, in fact, prevailingly signals attributable to the tetragonal 1:1 PdZn intermetallic alloy phase [32] and only a shoulder, detected at $2\theta = 40.1°$, is attributable to a very small amount of metallic Pd.

The diffraction pattern of the Pd/C catalyst, prepared in order to have a pure Pd(0) containing sample, presents the three peaks that are usually assigned to metallic Pd [32]. The dimension of the Pd particles is estimated to be $\approx$11 nm.

3.1.2. Trasmission electron microscopy (TEM)

The high resolution transmission electron micrographs of the HTZAPd373 and HTZAPd673 samples are shown in figures 3 and 4.

Only a small number of metallic particles with size in the range of 2–4 nm were found in the (HTZAPd373) sample reduced at the lower temperature. It is likely that the great majority of them are too small to be visible by this technique.

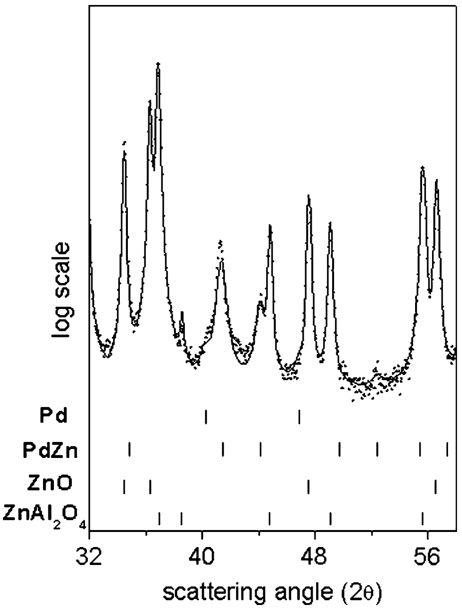

Figure 2. X-ray diffraction patterns (logarithmic scale) versus 2θ of HTZAPd673. Data points refer to experimental data and full lines to a curve fit according to the Rietveld methods.

On the other hand, the detected metallic particles were much more numerous in the HTZAPd673 sample reduced at higher temperature.

It is possible to assume that such particles, with dimension in the range of 5–8 nm, are composed by a PdZn phase even though it was not possible to confirm this assumption by EDS analysis because Zn is also present in the support oxides.

In the micrograph of HTZAPd673 one can see a very small number of particles with a core/shell structure (figure 5).

It is possible to hypothesize that the black core of this kind of particles is part of the Pd phase (2–4 nm), detected by XRD, while the surrounding shell can be a ZnO layer which is deposited on. The particles occluded inside the oxide shell will obviously be catalytically inactive.

3.2. Catalytic tests

The acetophenone hydrogenation process can be summarized by a quite complex reaction scheme (figure 6).

The reduction of the ketonic carbon-oxygen double bond gives 1-phenylethanol (PE), while the hydrogenation of the aromatic ring gives the cyclohexyl methyl ketone (CHMK). Both compounds can undergo further hydrogenation to 1-cyclohexylethanol (CHE). PE can further react to give ethyl benzene (EB) [16–28]. Hydrogenation of EB and CHE can generate ethylcyclohexane (EC).

The two Pd based catalysts (HTZAPd373, HTZAPd673) and Pd/C were tested in the acetophenone hydrogenation under the conditions described in the experimental section and in the 333–423 K temperature range. In all cases the main hydrogenation product was 1-phenylethanol (PE). At high temperatures ethyl benzene (EB) was also formed and traces of styrene were detected by GC-MS analysis (Table 1, 2, 3). Ethyl cyclohexane (EC) was found only in the case of Pd/C (Table 3).

Conversion and product distribution data, after 3 h of reaction time, for the catalyst HTZAPd373 are reported in Table 1

The catalyst shows a conversion of 44% at 333 K with a 98% selectivity to 1-phenyl ethanol. At 358 K the conversion increases to 71% and reaches the 99% at 423 K, but at the same time the selectivity to 1-phenylethanol (PE) decreases from 98% to 56% with the production of increasing amounts of ethyl benzene(EB). The formation of cyclohexylethanol (CHE) is 2% at all temperatures. At higher temperatures 1% of cyclohexyl methyl ketone (CHMK) was detected.

Totally different activity and selectivity values were found when the HTZAPd673 catalyst, reduced at higher

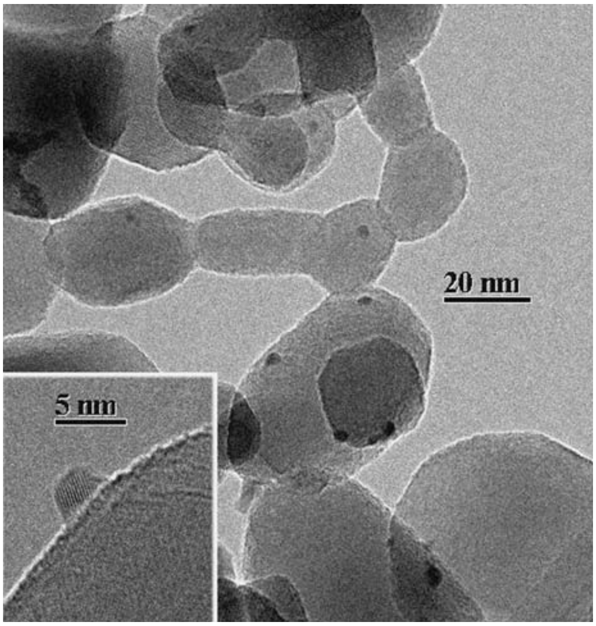

Figure 3. TEM micrograph of the HTZAPd373 sample; the darker dots are the metallic particles. The inset shows a HRTEM image of a single Pd particle with fringes due to the lattice planes.

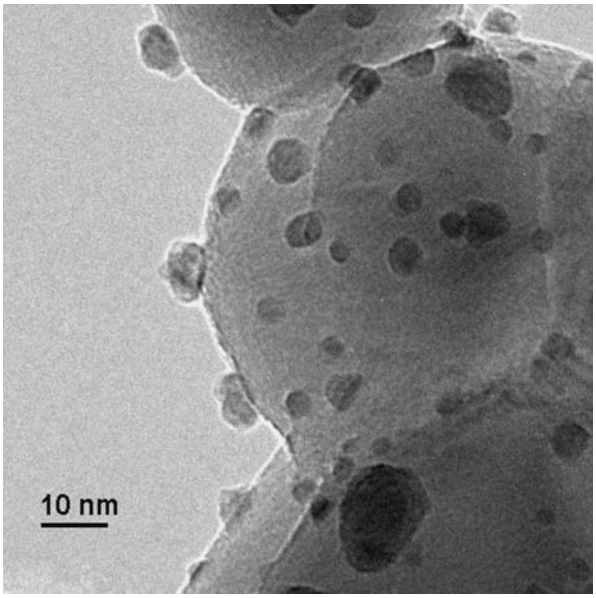

Figure 4. TEM micrograph of the HTZAPd673 sample. The darker dots are the PdZn alloy particles.

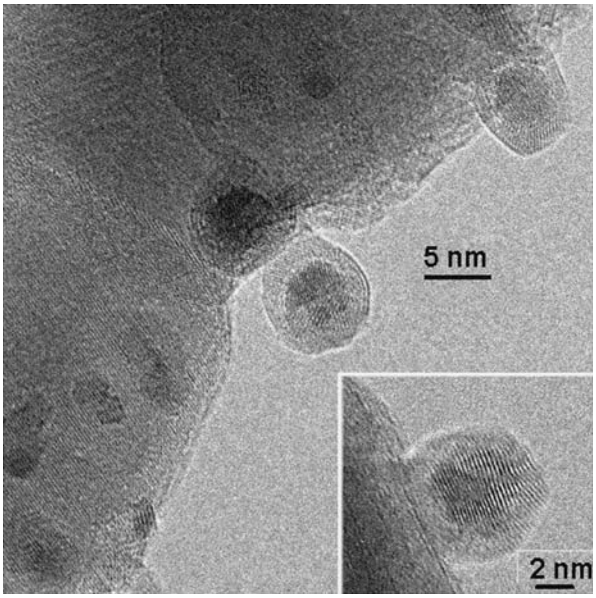

Figure 5. HRTEM images of some particles with a shell structure found in sample HTZAPd673.

temperatures, was used. The data after 3 h of reaction are reported in Table 2.

The conversion is only 10% at 333 K and increases up to 59% at 423 K, while the selectivity to phenyl ethanol (PE) remains constant in all the temperature ranges, with an average value of 97%. Cyclohexyl methyl ketone (CHMK) is the only by-product, but its formation declines with the increasing reaction temperature. At 423 K some (3%) ethyl benzene (EB) was detected.

Experimental data obtained with the Pd/C catalyst, summarized in Table 3, are similar to those found by other authors [25].

The catalytic activity of Pd/C resulted very high, with complete conversion of acetophenone even at 333 K. Ethyl benzene (EB) is the main product, above 358 K, and it is produced in a considerable amount even at low reaction temperatures. At 423 K a 9% of ethyl cyclohexane (EC) is also formed.

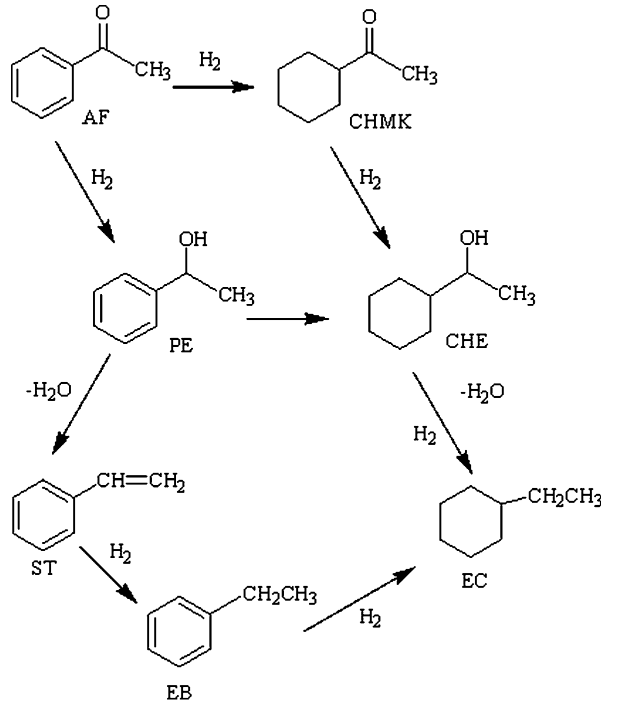

Figure 6. Reaction scheme for the hydrogenation of acetophenone. AP = acetophenone, PE = 1-phenilethanol, CHMK = methilcyclohexylketone, CHE = cyclohexylethanol, ST = Styrene, EB ethyl benzene, EC ethylcyclohexane.

Table 1

Product distribution and total conversion after 3 h of reaction over HTZAPd373 catalysts

T(K)	Conv.%	Products distribution %			
		PE	CHMK	CHE	EB
333	44	98	0	2	0
358	71	98	0	2	0
383	98	78	1	2	19
423	99	56	1	2	41

Table 2

Product distribution and total conversion after 3 h of reaction time over HTZAPd673 catalyst

T(K)	Conv.%	Products distribution %			
		PE	CHMK	CHE	EB
333	10	98	2	0	0
358	38	98	2	0	0
383	51	78	2	0	0
423	59	96	1	0	3

The different nature of the active metallic phase can explain the different catalytic performances of both Pd/C, which contains only metallic palladium, and of the two HTZAPd373 and HTZAPd673 samples, that were found to contain increasing amounts of Pd/Zn alloy.

Table 3

Product distribution and total conversion after 3 h of reaction time over Pd/C catalysts

T(K)	Conv.%	Products distribution %		
		PE	EB	EC
333	100	60	40	0
358	100	10	90	0
383	100	2	97	1
423	100	0	91	9

The electronic and chemical perturbations induced by the bonding of zinc to a late transition metal (Rh, Pt, Pd) have been the object of experimental and theoretical studies [34–37]. It was found [35] that a very good correlation exists between the strength of the bimetallic bonding and changes in the electronic and chemical properties of the metal. The stronger the bimetallic bond, the lower the ability of the late transition metal to bond CO because of a decrease in the metal-ligand back donation [35]. Various authors found that CO chemisorption drastically decreases when Pd is alloyed with Zn [36]. The PdZn alloy features a CuAu ($L1_0$ type) [33, 36] tetragonal structure and a computational study [36] showed that the local electronic structure of Pd in the PdZn alloy resembles that of Cu. The same authors [36] demonstrated that, due to the stronger Pd–Zn bonding, compared to the homonuclear Pd–Pd and Zn–Zn bonds, surface segregation of neither Zn nor Pd is favored. In the methanol steam reforming and related reactions [8–13] the catalytic behavior of systems, the active phase of which was found to be the PdZn alloy, further encourages the idea of a close structural and chemical similarity of the 1:1 tetragonal PdZn alloy and Cu. It was recently found [38] that the heterogeneous hydrogenation of aryl ketones occurs with a very high selectivity to the corresponding alcohols in batch conditions on a Cu/Al_2O_3 (Cu 8% w/w) catalyst. Our results can be interpreted in the light of all these findings.

The carbon supported catalyst Pd/C behaves as a typical palladium based system [25] and the acetophenone reduction occurs giving phenylethanol (PE) that is converted to ethylbenzene (EB) in a consecutive reaction. The conversion of PE to EB increases rapidly with the temperature and EB represents the only product at higher temperatures. The HTZAPd673 catalyst, where Pd is totally present as 1:1 PdZn alloy, appeared to be much less active than pure palladium Pd/C and produces 98% of phenyl ethanol (PE) with conversion values increasing from 10% at 333 K to 59% at 423 K. The catalyst is less able to effectively catalyze the formation of ethyl benzene (EB) by the hydrogenolysis of phenyethanol (PE) in comparison to the pure metallic palladium and analogously to the copper based systems [38]. The low conversion of the reaction can be explained, at least in part, by the fact that a certain amount of the metal particles are covered by a zinc oxide shell that prevent any contact of the active alloy phase with the incoming reagents molecules.

In the HTZAPd373 catalyst, reduced at lower temperatures, a metallic Pd phase cohesists with a certain amount of the 1:1 PdZn alloy. At low temperatures PE is selectively formed (98%) but the aromatic ring is also hydrogenated and a 2% of cyclohexyl ethanol (CHE) is formed. At higher reaction temperature the overall conversion reaches 99% but an increasing amount of CHE is converted by hydrogenolysis to EB. At 423 K the conversion is 99%, with a 56% of PE and 41% of EB. The selectivity pattern of this sample is attributable to the presence of intimately mixed nanostructured palladium and PdZn alloy phases.

4. Conclusions

Impregnation (2% w/w) with Pd nitrate of the oxides obtained by thermal treatment at 1173 K of Zn–Al hydrotalcite like, layered double hydroxide, followed by reduction in hydrogen flow, gives origin to a material that actively catalyzes the acetophenone reduction with hydrogen in batch conditions. This procedure allows the obtainment of very small metallic particles dispersed on the oxide mixture. The catalytic system showed an interesting selectivity to phenyl ethanol. This catalytic behavior, that is very different from that of metallic palladium, is due to the formation of a 1:1 PdZn tetragonal alloy by thermal treatment in reducing conditions. The formation of the alloy starts at relatively low temperatures of the thermal treatment and is highly favored by the close interaction of small metallic particles with the supporting oxide mixture.

Acknowledgments

Financial support from the MIUR (Ministero dell'Istruzione, Università e Ricerca) is gratefully acknowledged.

References

[1] M. Hudlický, *Reduction in Organic Chemistry* (Ellis Horwood Lmtd, NewYork, 1984).
[2] B. Cocq and F. Figueras, J. Mol. Catal. A Chemical 173 (2001) 117.
[3] A. Tungler and G. Fogassy, J. Mol. Catal. A Chemical 173 (2001) 231.
[4] P. Kačer, L.Červený, Appl. Catal. A, General, 229 (2002) 193 and references therein.
[5] P.S. Wehner and B.L. Gustafson, J. Catal. 135 (1992) 420.
[6] B.E. Green, C.S. Sass, L.T. Germinario, P.S. Wehner and B.L. Gustafson, J. Catal. 140 (1993) 406.
[7] N. Iwasa, O. Yamamoto, T. Akazawa, S. Ohyama and N. Takezawa, J. Chem. Soc. Chem. Commun. (1991) 1322.
[8] N. Iwasa, S. Masuda, N. Ogawa and N. Takezawa, Appl. Catal. A: General 125 (1995) 145.
[9] N. Iwasa, O. Yamamoto, R. Tamura, M. Nishikubo and N. Takezawa, Catal. Lett. 62 (1999) 179.
[10] Y.H. Chin, R. Dagle, J. Hu, A.C. Dohnalkova and Y. Wang, Catal. Today 77 (2002) 79.
[11] C.-T. Hong, C.-T. Yen and F.-H. Yu, Appl. Catal. 48 (1989) 385.
[12] A. Sarkany, Z. Zsoldos, B. Furlong, J.W. Hightower and L. Guczi, J. Catal. 141 (1993) 566.
[13] Z. Zsoldos, A. Sarkany and L. Guczi, J. Catal. 145 (1994) 235.
[14] F. Cavani, F. Trifirò and A. Vaccari, Catal.Today 11 (1991) 173.
[15] F. Trifirò and A. Vaccari, in: *Comprehensive Supramolecular Chemistry*, Vol. 7, eds. G. Alberti and T. Bein (Pergamon, New York, 1996) p. 251.
[16] B.F. Sels, D.E. De Vos and P.A. Jacobs, Cat. Rev. 43 (2001) 443.
[17] M.V. Rajashekharam, I. Bergault, P. Foilloux, D. Schweich, H. Delmas and R.V. Chaudhari, Catal. Today 48 (1999) 83.
[18] M.A. Aramendia, V. Borau, C. Jiménez, J.M. Marinas, M.E. Sempere and P. Urbano, Appl. Catal 43 (1988) 41.
[19] P.S. Kumbhar, Appl. Catal. A, General 96 (1993) 241.
[20] I. Bergault, P. Fouilloux, C. Joly-Vuillemin and H. Delmas, J. Catal. 175 (1998) 328.
[21] N. Lavaud, P. Magnoux, F. Alvarez, L. Melo, G. Giannetto and M. Guisnet, J. Mol. Catal. A Chemical 142 (1999) 223.
[22] I. Bergault, C. Joly-Vuillemin, P. Fouilloux and H. Delmas, Catal. Today 48 (1999) 161.
[23] S. Hamar-Thibault, J. Masson, P. Fouilloux and J. Court, Appl. Catal. A, General 99 (1993) 131.
[24] C.S. Chen, H.W. Chen, W.H. Cheng, Appl. Catal. A, General, 248 (2003) 117 and references therein.
[25] C.S. Chen and H.W. Chen, Appl. Catal. A, General 260 (2004) 207.
[26] J. Masson, S. Vidal, P. Cividino, P. Fouilloux and J. Court, Appl. Catal. A, General 99 (1993) 147.
[27] R.V. Malyala, C.V. Rode, M. Arai, S.G. Hedge and R.V. Chaudari, Appl. Catal. A, General 193 (2000) 71.
[28] M. Casagrande, L. Storaro, A. Talon, M. Lenarda, R. Frattini, E. Rodriguez-Castellón and P. Maireles-Torres, J. Mol. Catal. A 188 (2002) 133.
[29] G.F. Sartori, A.G. Maglioni, V. Vetere, G.Y. Moltrasio Iglesias, M.L. Casella and O.P.A. Ferretti, Appl. Catal. A, General 269 (2004) 215.
[30] U. Costantino, F. Marmottini, M. Nocchetti, and R. Vivani, Eur. J. Inorg. Chem. (1998) 1439.
[31] R.A. young Ed. *The Rietveld Method* (International Union of Crystallography, Oxford University Press, Oxford 1993).
[32] L. Lutterotti and S. Gialanella, Acta Mater. 46 (1998) 101.
[33] International Centre for Diffraction Data-JCPDS (JCPDS 46–1043).
[34] J.A. Rodriguez, J. Phys. Chem. 98 (1994) 5758.
[35] J.A. Rodriguez and M. Kuhn, J.Phys.Chem. 100 (1996) 381 and references therein.
[36] Z.X. Chen, K.M. Neyman, A.B. Gordienko and N. Rösch, Phys. Rev. B 68 (2003) 75417.
[37] Z.X. Chen, K.M. Neyman, K.W. Lim and N. Rösch, Langmuir 20 (2004) 8068.
[38] F. Zaccheria, N. Ravasio, R. Psaro and A. Fusi, Tetrahedron Lett. 46 (2005) 3695.